A Multiparameter Moment-Matching Model-Reduction Approach for Generating Geometrically Parameterized Interconnect Performance Models

Luca Daniel, *Member, IEEE*, Ong Chin Siong, Low Sok Chay, Kwok Hong Lee, and Jacob White, *Associate Member, IEEE*

***Abstract*—In this paper, we describe an approach for generating accurate geometrically parameterized integrated circuit interconnect models that are efficient enough for use in interconnect synthesis. The model-generation approach presented is automatic, and is based on a multiparameter moment matching model-reduction algorithm. A moment-matching theorem proof for the algorithm is derived, as well as a complexity analysis for the model-order growth. The effectiveness of the technique is tested using a capacitance extraction example, where the plate spacing is considered as the geometric parameter, and a multiline bus example, where both wire spacing and wire width are considered as geometric parameters. Experimental results demonstrate that the generated models accurately predict capacitance values for the capacitor example, and both delay and cross-talk effects over a reasonably wide range of spacing and width variation for the multiline bus example.**

***Index Terms*—Interconnect synthesis, integrated circuits interconnections, modeling, parameterized reduced-order systems, reduced-order systems.**

I. Introduction

DEVELOPERS of routing tools for mixed-signal applications could make productive use of more accurate performance models for interconnect, but the cost of extracting even a modestly accurate model for a candidate route is far beyond the computational budget of the inner loop of a router. If it were possible to extract geometrically parameterized, but inexpensive to evaluate, models for the interconnect performance, then such models could be used for detailed interconnect synthesis in performance critical digital or analog applications.

The idea of generating parameterized reduced-order interconnect models is not new. Recent approaches have been developed that focus on statistical performance evaluation [1], [2] and clock-skew minimization [3]. However, our target application, interconnect synthesis, requires parameterized models valid over a wide geometric range. Generating such parameterized models is made difficult by the fact that even though the electrical behavior of interconnect can be modeled by a linear time-invariant dynamical system, that system typically depends nonlinearly on geometric parameters.

One recently developed technique for generating geometrically parameterized models of physical systems assumed a linear dependence on the parameter, and was applied to reducing a discretized linear partial differential equation [4]. The approach used closely paralleled the techniques used for dynamic system-model reduction, an unsurprising fact given that if the parameter dependence is linear, the generated parameterized system of equations is structurally identical to a Laplace transform description of a linear time-invariant dynamical system, though the frequency variable is in the place of the geometric parameter.

The observation that geometric parameters and frequency variables are interchangeable, at least when the dependence of the geometric variation is linear, suggests that the parameterized reduction problem could be formulated so as to make use of extensions to the projection-subspace-based moment-matching methods that have proved so effective in interconnect modeling [5]–[13]. In this paper, we develop approaches for generating parameterized interconnect models exploiting just such a connection. We start in Section II by examining the single geometric parameter case, and treat the case when the variation with respect to the geometric parameter is nonlinear. In Section III, we apply the single-parameter approaches to the problem of automatically extracting parameterized models for interconnect capacitances from integral equation-based capacitance-extraction techniques. In Section IV, we present a more general problem formulation for an arbitrary number of parameters. In Section V, we extend the two-parameter moment-matching model-reduction technique in [14], introducing a moment-matching model-reduction algorithm for an arbitrary number of parameters. In the same section, we also derive a rigorous proof for the moment-matching properties of our algorithm. In Section VI, we analyze the complexity of the algorithm in terms of model-order growth as a function of the number of parameters, and the cost of the model construction

Manuscript received June 1, 2002; revised December 25, 2002. This work was supported in part by the Singapore-MIT Alliance, in part by the Semiconductor Research Corporation, and in part by the DARPA NeoCAD Program managed by the Sensors Directorate of the Air Force Laboratory, USAF, Wright-Patterson AFB. This paper was recommended by Associate Editor C. J. Alpert.

L. Daniel and J. White are with the Department of Electrical Engineering and Computer Science, Massachusetts Institute of Technology, Cambridge, MA 02139 USA (e-mail: luca@mit.edu; white@mit.edu).

O. C. Siong was with the National University of Singapore, Singapore 117576. He is now with Digisafe Pte Ltd., Singapore 609602.

L. S. Chay was with the National University of Singapore, Singapore. She is now with the Defense Science and Technology Agency, Singapore.

K. H. Lee was with the National University of Singapore, Singapore.

Digital Object Identifier 10.1109/TCAD.2004.826583

as a function of the size of the original system. In Section VII, we demonstrate the practical effectiveness of the method on a wire-spacing parameterized multiline bus example, and consider both delay and cross-talk effects. In Section VIII, we use the generalized multiparameter model-reduction approach to re-examine the multiline-bus example, but now allow both wire width and wire spacing, together with frequency to be parameters. Finally, conclusions are given in Section IX.

II. Single-Parameter Case

In this section, we consider the single-parameter case and, in Section III, we will use the resulting algorithm to generate parameterized formulas for interconnect-coupling capacitances. In examining this simpler case, we hope to clarify some of the issues that will arise in multiparameter reduction and better establish the connections between our approach with work by others.

To begin, consider a single-parameter linear system

$$\begin{aligned} E(s)x &= Bu \\ y &= Cx \end{aligned} \tag{1}$$

where s is the parameter; x is the vector of "states," a term we use loosely because s is not necessarily the Laplace frequency parameter, and the system in (1) is a "dynamical system in state space form," only when s is the Laplace frequency parameter. Vectors u and y are t-dimensional input and output vectors; $E(s)$ is an $n \times n$ matrix; and B and C are $n \times t$ and $t \times n$ matrices, which define how the inputs and outputs relate to the state vector x.

For many interconnect problems, the number of inputs and outputs t is typically much smaller than n, the number of states needed to accurately represent the electrical behavior of the interconnect. In order to generate a representation of the input-output behavior given by (1) using many fewer states, a projection approach is commonly used [8]. In the projection approach, one first constructs an $n \times q$ projection matrix V, where $q \ll n$, and then one generates the reduced model from the original system using congruence transformations [7]. Specifically, the reduced system is given by

$$\begin{aligned} \left[V^T E(s) V\right] \hat{x} &= V^T B u \\ y &= CV\hat{x} \end{aligned} \tag{2}$$

where the reduced-state vector $\hat{x}$ is of dimension q and is representing the projection of the large original state vector $x \approx V\hat{x}$. Note that the columns of V are typically chosen in such a way that the final response of the reduced system matches q terms in the Taylor series expansion in s of the original response, regardless if s is a Laplace frequency parameter or instead some other kind of geometrical parameter.

The reduced-order system given in (2) is not really an efficient reduced model, as explicit evaluation of $V^T E(s) V$ requires order n^2 operations if $E(s)$ is dense and nq operations if $E(s)$ is sparse. To generate a reduced model that can be more efficiently evaluated, consider using polynomial interpolation or a Taylor series expansion to generate a representation of $E(s)$ that can be expressed as a power series

$$E(s) = \sum_{m=0}^{\infty} s^m E_m. \tag{3}$$

There are several approaches for constructing a reduced-order model, given the $E(s)$ in (3). If the power series is truncated to order p, it is possible to transform the power-series reduction problem to a p-parameter reduction problem, with only a linear dependence on the newly introduced parameters $s_m = s^m, m = 1, \ldots, p$, as in

$$E(s) \approx E_0 + s_1 E_1 + s_2 E_2 + \cdots + s_p E_p. \tag{4}$$

After this transformation, the multiparameter algorithms which will be described in Section V can be used directly, though the dimension of the resulting reduced model may be unnecessarily high.

A more efficient reduction approach can be derived by converting (1) to a linear single-parameter reduction problem by introducing fictitious states [15]. The resulting representation of $E(s)$ is linearly dependent on s and is given by

$$\left\{ \begin{bmatrix} E_0 & & & \\ & I & & \\ & & I & \\ & & & \ddots \end{bmatrix} - s \begin{bmatrix} -E_1 & -E_2 & -E_3 & \cdots \\ I & & & \\ & I & & \\ & & \ddots & \end{bmatrix} \right\} \times \begin{bmatrix} x \\ x_1 \\ x_2 \\ \vdots \end{bmatrix} = \begin{bmatrix} B \\ 0 \\ 0 \\ \vdots \end{bmatrix} u \tag{5}$$

where the fictitious states, denoted x_i, satisfy the relation

$$x_1 = sx \quad x_2 = sx_1 \quad x_3 = sx_2 \quad \ldots.$$

Examination of (5) yields a series expansion for x in terms of the parameter s. That is,

$$x = \sum_{m=0}^{\infty} s^m F^m \tag{6}$$

where

$$F^m = -\sum_{k=0}^{m-1} E_0^{-1} E_{m-k} F^k, \qquad m > 0 \tag{7}$$

and

$$F^0 = E_0^{-1} B. \tag{8}$$

The projection matrix used to generate a qth reduced-order model is then given by

$$\mathrm{colspan}(V) \supseteq \mathrm{span}\{F^0, F^1, \ldots, F^{q-1}\}$$

and the reduced model is

$$\begin{aligned} \left(\sum_{m=0}^{p} V^T E_m V s^m \right) \hat{x} &= V^T B u \\ y &= CV\hat{x}. \end{aligned} \tag{9}$$

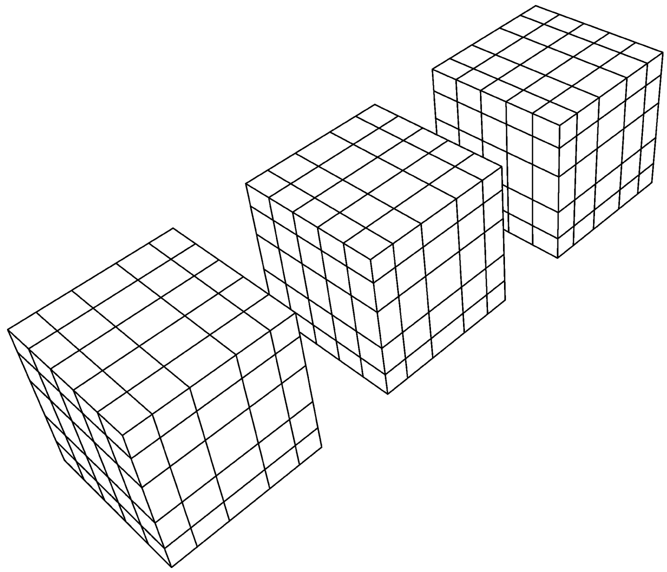

Fig. 1. Three conductors example for capacitance extraction. Conductors are $1 \times 1 \times 1$ m. Nominal gap is 0.5 m. The discretization of the surface into small panels is also shown.

III. Parameterized Capacitance Extraction

In this section, we use the single-parameter model-reduction strategy described above to generate parameterized models for interconnect self and coupling capacitances. We start with a brief description of the capacitance-extraction problem, and then describe how we made use of the model reduction.

A. Computing Capacitances

Consider the three conductors example in Fig. 1, in which we are interested in determining the relation between the coupling capacitances and the conductor separation distances. The matrix of self and coupling capacitances is usually computed by solving an integral equation for the conductor surface charges, and then integrating those charges to determine conductor capacitances. In particular, the surface-charge density σ must satisfy the first-kind integral equation

$$\psi(r) = \int_{\text{surfaces}} \sigma(r') \frac{1}{4\pi\varepsilon_0 \|r - r'\|} da' \tag{10}$$

where r and r' are positions on the conductor surfaces, $\psi(r)$ is the known conductor surface potential, da' is the incremental conductor surface area, and $\|r\|$ is the usual Euclidean length of r.

A standard approach to numerically solving (10) for σ is to use a piece-wise constant collocation scheme. In such schemes, the conductor surfaces are divided up into n small panels, and σ is assumed constant on each panel, thus generating a piecewise constant approximation to σ. The n panel charges can then be determined by insisting that the approximation to σ generates the correct potential at n test points located at the centroids of the n panels. This constraint on the panel charges can be represented as a linear system of equations

$$Ex = b \tag{11}$$

where E is the dense matrix, which relates unknown panel charges to known panel potentials, x is the vector of panel charges, $b \in \mathbf{R}^n$ is the vector of known panel centroid potentials, and

$$E_{ij} = \frac{1}{a_j} \int_{\text{panel}_j} \frac{1}{4\pi\varepsilon_0 \|r_i - r'\|} da' \tag{12}$$

where r_i is the centroid of the ith panel and a_j is the area of the jth panel.

For the three-conductor example shown in Fig. 1, there are a total of six coupling capacitances and three self capacitances. To determine these capacitance values, one can solve (11) three times, with three different b vectors. Specifically, the three different b vectors are used to set a nonzero voltage on only one conductor at a time. Weighted combinations of the three computed vectors of panel charges x then yield the self and coupling capacitances. Altering the spacing between the three conductors will change the separation distances between pairs of panels and centroids that reside on different conductors. As is clear from the formula for the potential coefficients, (12), the coefficients E_{ij} depend nonlinearly on the panel separation distances and, therefore, the matrix E depends nonlinearly on conductor separation distances.

B. Approximating the Potential Coefficient Matrix

In order to apply the above techniques for model reduction to the capacitance-extraction problem, it is first necessary to generate a polynomial approximation for the variations in the potential coefficient matrix E caused by variations in separation distance w. For the three conductors example in Fig. 1, we used both a Taylor series and Chebyshev polynomial interpolation approaches to generate a quadratic approximation of the form

$$E(w) \approx E_0 + wE_1 + w^2 E_2$$

where note that E_0, E_1, and E_2 are $n \times n$ matrices. After the polynomial coefficients are obtained, they can be used in the recursion formula (7) to generate V, which can in turn be used to obtain a reduced system. Hence,

$$\begin{aligned}
&E(w)x = b\\
&\quad\Downarrow \text{Taylor or Chebyshev approximation}\\
&(E_0 + wE_1 + w^2E_2)\hat{x} = b\\
&\quad\Downarrow \text{Model Order Reduction}\\
&\qquad \text{through recursion formula}\\
&V^T(E_0V + wV^TE_1V + w^2V^TE_2V)\hat{x} = V^Tb.
\end{aligned}$$

Example-capacitance results for the three conductors example are shown in Figs. 2 and 3. The conductors were discretized into approximately 600 panels, (12) was used to compute the $E(w)$ matrix, and (11) was solved to determine normalized self and coupling capacitances for the conductors. In addition, $E(w)$ was fit with a quadratic expansion in w using a Taylor series and a Chebyshev expansion, then these expanded matrices were reduced, as described above.

In Fig. 2, the self and coupling capacitances computed using the exact $E(w)$ are compared to those produced using quadratic models generated using the Taylor and Chebyshev approximations (no model reduction was applied). As is clear from the figure, the quadratic approximations fit reasonably well from one fifth of the nominal gap spacing to nearly twice the gap

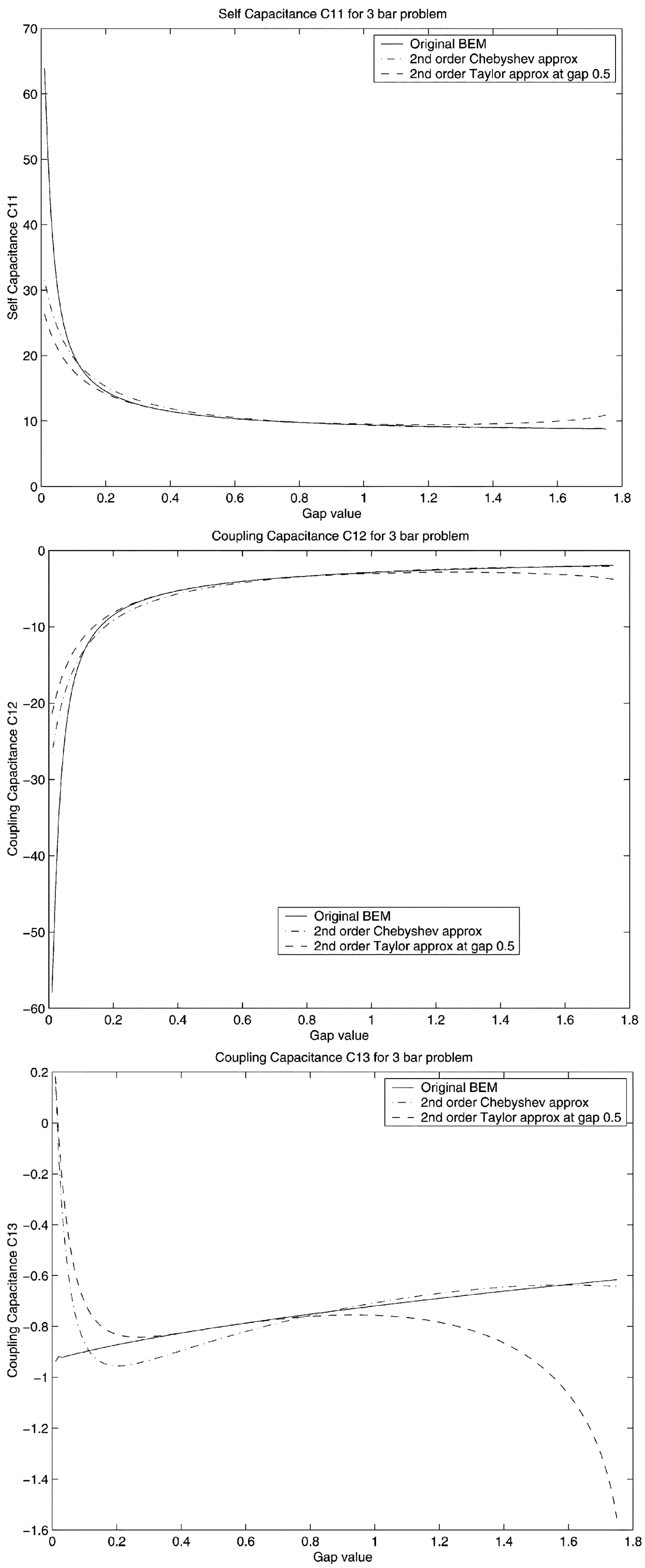

Fig. 2. Illustration of the error introduced by the first step of our procedure. In this example, an approximation using second-order Taylor or Chebyshev polynomials. Taylor is better locally around its expansion point $(\mathrm{gap} = 0.5\ \mathrm{m})$, while Chebyshev is better on a wider range of values, yet still finite (e.g., see lower plot). No model-order reduction technique has been applied at this stage. Capacitances values should be scaled by 10 pF, gap is in m.

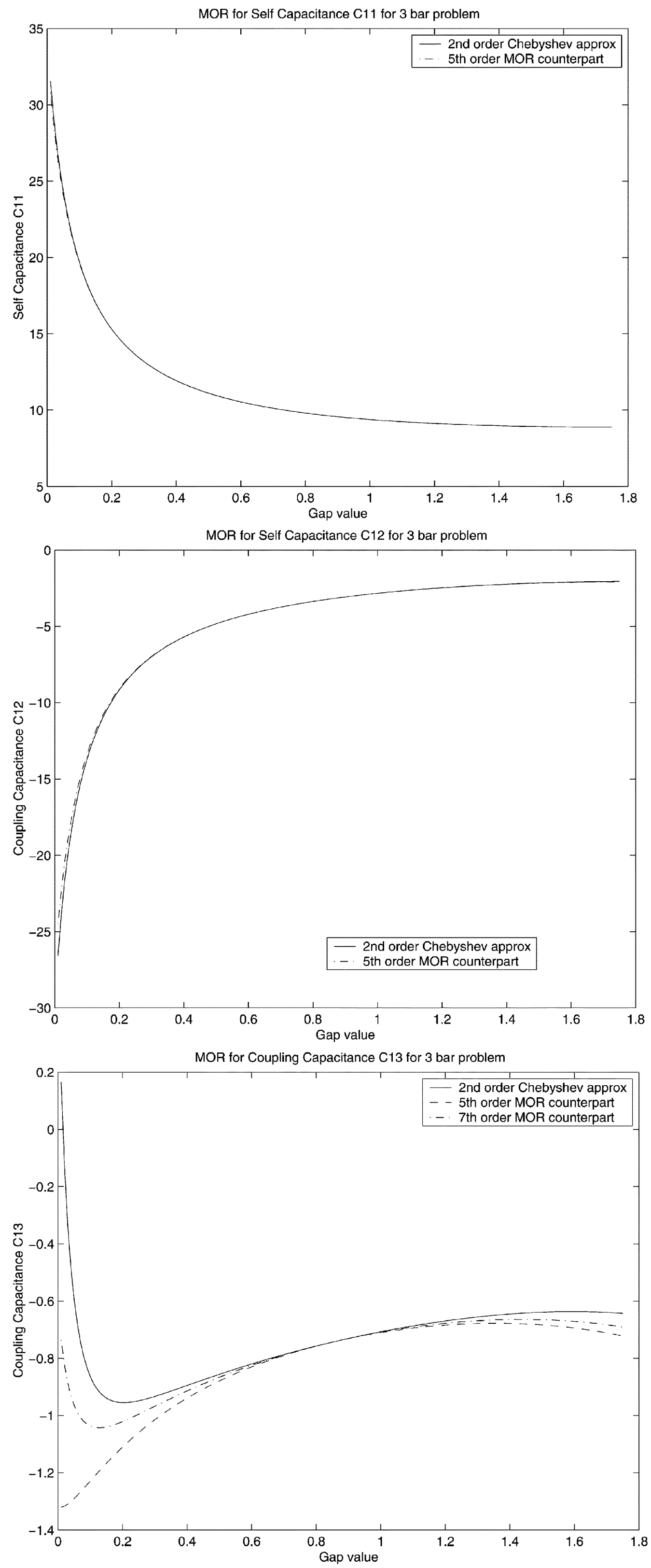

Fig. 3. Illustration of the additional error introduced by the actual model-order reduction step (second step). The reference for the comparison in this figure is the result of the first step: the second-order Chebyshev approximation. The reduction step produces a good fit around the expansion point. However, the model is valid only for a finite range of values of the parameter. Higher orders are shown to yield higher accuracies and wider ranges. Capacitance values should be scaled by 10 pF, gap is in m.

spacing. Both the Taylor and Chebyshev methods become inaccurate for very small conductor separations, and the Chebyshev method is more accurate for large separations, being indistinguishable from the exact $E(w)$ solution at 1.8 times the nominal spacing, at least for the self and largest coupling capacitance. Note that the capacitance coupling for the first and third conductor is an order of magnitude smaller than the self and nearby coupling capacitances, but is still approximated reasonably accurately.

In order to examine the impact on accuracy of the model reduction, the three 600×600 matrices generated by the quadratic Chebyshev expansion were reduced to 5×5 and 7×7 matrices using the congruence-projection model-reduction described above. Once the reduced matrices are calculated, evaluating the self and coupling capacitances for a new value of w is just a matter of a few very simple additions and factorizations operations on matrices of order 5×5 or 7×7. As shown in Fig. 3, the capacitances computed using the original 600×600 Chebyshev matrices are indistinguishable from those generated by the reduced models for the self and nearby coupling capacitances. In addition, the reduced model results are still reasonable for the much smaller distance coupling capacitance.

IV. More General Problem Formulation

When modeling long-interconnect wires, it is usually insufficiently accurate to use a simple-lumped capacitor model. Instead, the long wires are usually modeled using a distribution of resistors and capacitors, and sometimes even inductors. Even if there is only one geometric parameter of interest, such interconnect examples still generate a multiparameter reduction problem, with frequency being the second parameter.

In order to derive an approach for the multiparameter problem, consider the following parameterized state space system model:

$$\begin{aligned} E(s_1, \ldots, s_\mu)x &= Bu \\ y &= Cx \end{aligned} \tag{13}$$

where $s_1, \ldots, s_\mu$ are μ parameters, x is the state of the system, $E(s_1, \ldots, s_\mu) \in \mathbf{R}^{n \times n}$ is the system descriptor matrix, B is a matrix relating the inputs u to the state x, and C is a matrix relating the state to the outputs y.

In general, the descriptor matrix $E(s_1, \ldots, s_\mu)$ could have a complicated and nonlinear dependence on the parameters $s_1, \ldots, s_\mu$. As a first step of our approach, we capture this dependence by means of a power series in the parameters $s_1, \ldots, s_\mu$

$$\begin{aligned} E(s_1, \ldots, s_\mu) = E_0 + \sum_i s_i E_i + \sum_{h,k} s_h s_k E_{h,k} \\ + \sum_{h,k,j} s_h s_k s_j E_{h,k,j} + \cdots \end{aligned} \tag{14}$$

One of the easiest ways to produce such a power-series representation is to truncate the μ variables Taylor-series expansion shown in (15) (see equations (15)–(18) at the bottom of the page), where $\bar{s}_1, \ldots, \bar{s}_\mu$ are the expansion points. In a practical implementation, one could, for instance, choose the expansion points to coincide with the "nominal values" for each of the parameters. Also, in practical implementations one could be more interested in working explicitly with variables that represent relative variations $\Delta s_i / \bar{s}_i$ of the actual parameters around the expansion points, rather than working with absolute variations Δs_i. Finally, as an alternative to using a μ-variables Taylor-series expansion, it is also possible to generate the power-series representation using, instead, polynomial interpolation to a set of data points.

$$\begin{aligned} &E(s_1, \ldots, s_\mu) \\ &\quad = E(\bar{s}_1, \ldots, \bar{s}_\mu) + \sum_i \left(\frac{\Delta s_i}{\bar{s}_i}\right) \left[\bar{s}_i \frac{\partial E}{\partial s_i}(\bar{s}_1, \ldots, \bar{s}_\mu)\right] + \sum_{h,k} \left(\frac{\Delta s_h}{\bar{s}_h}\right)\left(\frac{\Delta s_k}{\bar{s}_k}\right) \left[\bar{s}_h \bar{s}_k \frac{\partial^2 E}{\partial s_h \partial s_k}(\bar{s}_1, \ldots, \bar{s}_\mu)\right] + \cdots \end{aligned} \tag{15}$$

$$\left[V^T E_0 V + \sum_i s_i V^T E_i V + \sum_{h,k} s_h s_k V^T E_{h,k} V + \sum_{h,k,j} s_h s_k s_j V^T E_{h,k,j} V + \cdots \right] x = V^T B u, \quad y = CVx \tag{16}$$

$$\left\{ I - \left[\sum_i s_i (-E_0^{-1}) E_i + \sum_{h,k} s_h s_k (-E_0^{-1}) E_{h,k} + \sum_{h,k,j} s_h s_k s_j (-E_0^{-1}) E_{h,k,j} + \cdots \right] \right\} x = E_0^{-1} B u \tag{17}$$

$$\begin{aligned} x &= \left\{ I - \left[\sum_i s_i \left(-E_0^{-1}\right) E_i + \sum_{h,k} s_h s_k \left(-E_0^{-1}\right) E_{h,k} + \sum_{h,k,j} s_h s_k s_j \left(-E_0^{-1}\right) E_{h,k,j} + \cdots \right] \right\}^{-1} E_0^{-1} B u \\ &= \sum_{m=0}^{\infty} \left[\sum_i s_i \left(-E_0^{-1}\right) E_i + \sum_{h,k} s_h s_k \left(-E_0^{-1}\right) E_{h,k} + \sum_{h,k,j} s_h s_k s_j \left(-E_0^{-1}\right) E_{h,k,j} + \cdots \right]^m E_0^{-1} B u \end{aligned} \tag{18}$$

Given the power-series representation in (14), a reduced-order model can then be generated by using a congruence transformation on the power-series representation, as in (16), where $V \in \mathbf{R}^{n\times q}$, and the size q of the reduced-order system matrices is typically much smaller than the size n of the original system matrices.

In order to calculate the column span of the projection matrix V, it is convenient to use the power series (14) to rewrite system (13) as in (17), so that x is given by (18).

V. P Parameter Model-Order Reduction

One simple way to construct the columns of the projection matrix V for the reduced order model in (16) is to identify a new set of parameters $\tilde{s}_i$ and matrices $\tilde{E}_i$ (see equation (16) at the bottom of the previous page),

$$\tilde{E}_i = \begin{cases} E_i & i=0,\ldots,\mu \\ E_{h,k} & h=1,\ldots,\mu;\;\; k=1,\ldots,\mu \\ E_{h,k,j} & h=1,\ldots,\mu;\;\; k=1,\ldots,\mu\; j=1,\ldots,\mu \\ \ldots \end{cases}$$
$$\tilde{s}_i = \begin{cases} s_i & i=1,\ldots,\mu \\ s_h s_k & h=1,\ldots,\mu;\;\; k=1,\ldots,\mu \\ s_h s_k s_j & h=1,\ldots,\mu;\;\; k=1,\ldots,\mu\; j=1,\ldots,\mu \\ \ldots \end{cases}$$

so that one can rewrite the parameterized system in (13) as a linearly parameterized model

$$\begin{aligned} \left[\tilde{E}_0 + \tilde{s}_1\tilde{E}_1 + \cdots + \tilde{s}_p\tilde{E}_p\right] x &= Bu \\ y &= Cx. \end{aligned} \tag{19}$$

In the special case [(20) and (21)], the power series is constructed using a Taylor series expansion. [See equations (20) and (21) at the bottom of the page.] In this simplified setting, the reduced model is now

$$\begin{aligned} \left[V^T\tilde{E}_0V + \tilde{s}_1V^T\tilde{E}_1V + \cdots + \tilde{s}_pV^T\tilde{E}_pV\right]\hat{x} &= V^TBu \\ y &= CV\hat{x} \end{aligned} \tag{22}$$

and once again, in order to calculate the column span of the projection matrix V, it is convenient to write the system (19) as

$$\begin{aligned} \left[I - (\tilde{s}_1M_1 + \cdots + \tilde{s}_pM_p)\right] x &= B_Mu \\ y &= Cx \end{aligned}$$

where

$$\begin{aligned} M_i &= -\tilde{E}_0^{-1}\tilde{E}_i \quad \text{for } i=1,2,\ldots,p \\ B_M &= \tilde{E}_0^{-1}B. \end{aligned}$$

Hence, x is given by (23) [See equations (23)–(27) at the bottom of the next page.]

Lemma 1: The coefficients $F^m_{k_2,\ldots,k_p}(M_1,\ldots,M_p)$ of the series in (23) can be calculated using (24).

The proof can be found in Appendix A. For a single input system, $B_M = b_M = \tilde{E}_0^{-1}b \in \mathbf{R}^{n\times 1}$, and the columns of V can be constructed to span the Krylov subspace (25), or equivalently (26).

The following lemmas are useful to prove the main moment matching theorem for parameterized model order reduction.

Lemma 2: If V is an orthonormal matrix $V \in \mathbf{R}^{n\times q}$, $V^TV = I_q \in \mathbf{R}^{q\times q}$, and z is any vector in the column span of the matrix V, $z \in \mathrm{colspan}(V)$, then $VV^Tz = z$.

Note that "in general" $VV^T \neq I_n \in \mathbf{R}^{n\times n}$.

Lemma 3: If V is an orthonormal matrix $V \in \mathbf{R}^{n\times q}$, $V^TV = I_q$, and z is a vector such that $\tilde{E}_0^{-1}z \in \mathrm{colspan}(V)$, then $(V^T\tilde{E}_0V)^{-1}V^Tz = V^T\tilde{E}_0^{-1}z$.

Lemma 4: If $F^m_{k_2,\ldots,k_p}(M_1,\ldots,M_p)$ is a matrix constructed as in (24), and $V \in \mathbf{R}^{n\times q}$ is an orthonormal matrix constructed such that (26) holds, then (27) holds for $m = 0,1,\ldots,m_q$.

Theorem 1: (*Parameterized Model Order Reduction Moment Matching Theorem*) The first q moments (corresponding to the first m_q orders of derivatives in each parameter) of the transfer function for the reduced-order model (22), constructed using the q columns of the orthonormal projection matrix $V \in \mathbf{R}^{n\times q}$ in (26) match the first q moments (corresponding to the first m_q orders of derivatives in each parameter) of the transfer function of the original system (19).

Proofs for Lemma 2–4 and for Theorem 1 are given in Appendices B–E, respectively. Note that the development closely follows the two-parameter approach given in [14].

$$\tilde{E}_0 = E(\bar{s}_1,\ldots,\bar{s}_p) \tag{20}$$

$$\tilde{E}_i = \begin{cases} \left[\bar{s}_i\frac{\partial E}{\partial s_i}(\bar{s}_1,\ldots,\bar{s}_p)\right] & i=1,\ldots,\mu \\ \left[\bar{s}_h\bar{s}_k\frac{\partial^2 E}{\partial s_h\partial s_k}(\bar{s}_1,\ldots,\bar{s}_p)\right] & h=1,\ldots,\mu;\;\; k=1,\ldots,\mu \\ \ldots \end{cases}$$
$$\tilde{s}_i = \begin{cases} \left(\frac{\Delta s_i}{\bar{s}_i}\right) & i=1,\ldots,\mu \\ \left(\frac{\Delta s_h}{\bar{s}_h}\right)\left(\frac{\Delta s_k}{\bar{s}_k}\right) & h=1,\ldots,\mu;\;\; k=1,\ldots,\mu \\ \ldots \end{cases}. \tag{21}$$

Extension of the parameterized model-order reduction moment matching theorem to multi-input systems is straightforward. For a t-input system, the columns of V can be constructed to span the Krylov subspaces produced by all the columns $[b_M]_j$ of B_M as shown in (28).

VI. Order Growth and Computational Complexity Analysis

Lemma 5: If p is the total number of parameters and m_q is the largest order of derivative that will be matched with respect to any parameter, then the order q of the parameterized reduced system is

$$q = O\left(\frac{p^{m_q}}{m_q^{m_q-(1/2)}}\right)$$

(proof in Appendix F).

One way to improve accuracy is to increase m_q. Unfortunately, with large m_q the order of the produced model might quickly become impractical. When $m_q = 1$, the order of the produced model scales linearly with the number of parameters and a large number of parameters can be handled. In some applications, the accuracy given by matching a single derivative per parameter can be good enough. In particular, we recall that many of the examples presented in this paper are obtained using

$$\begin{aligned} x &= [I - (\tilde{s}_1 M_1 + \cdots + \tilde{s}_p M_p)]^{-1} B_M u = \sum_{m=0}^{\infty} [\tilde{s}_1 M_1 + \cdots + \tilde{s}_p M_p]^m B_M u \\ &= \sum_{m=0}^{\infty} \sum_{k_2=0}^{m-(k_3+\cdots+k_p)} \cdots \sum_{k_{p-1}=0}^{m-k_p} \sum_{k_p=0}^{m} \left[F^m_{k_2,\ldots,k_p}(M_1,\ldots,M_p) B_M u\right] \tilde{s}_1^{m-(k_2+\cdots+k_p)} \tilde{s}_2^{k_2} \ldots \tilde{s}_p^{k_p} \end{aligned} \tag{23}$$

$$\begin{aligned} &F^m_{k_2,\ldots,k_p}(M_1,\ldots,M_p) \\ &= \begin{cases} 0, & \text{if } k_i \notin \{0,1,\ldots,m\} i = 2,\ldots,p \\ 0, & \text{if } k_2 + \cdots + k_p \notin \{0,1,\ldots,m\} \\ I, & \text{if } m = 0 \\ M_1 F^{m-1}_{k_2,\ldots,k_p}(M_1,\ldots,M_p) + M_2 F^{m-1}_{k_2-1,\ldots,k_p}(M_1,\ldots,M_p) + \cdots & \\ \quad \cdots + M_p F^{m-1}_{k_2,\ldots,k_p-1}(M_1,\ldots,M_p) & \end{cases} \end{aligned} \tag{24}$$

$$\begin{aligned} &\operatorname{colspan}(V) \\ &= \operatorname{span}\Big\{ b_M, M_1 b_M, M_2 b_M, \ldots, M_p b_M, M_1^2 b_M, (M_1 M_2 + M_2 M_1) b_M, \ldots, \\ &\qquad (M_1 M_p + M_p M_1) b_M, M_2^2 b_M, (M_2 M_3 + M_2 M_3) b_M, \ldots \Big\}, \end{aligned} \tag{25}$$

$$= \operatorname{span}\left\{ \bigcup_{m=0}^{m_q} \bigcup_{k_2=0}^{m-(k_p+\cdots+k_3)} \cdots \bigcup_{k_{p-1}=0}^{m-k_p} \bigcup_{k_p=0}^{m} F^m_{k_2,\ldots,k_p}(M_1,\ldots,M_p) b_M \right\}. \tag{26}$$

$$\begin{aligned} &\hat{F}^m_{k_2,\ldots,k_p}\left[-\left(V^T\tilde{E}_0 V\right)^{-1} V^T \tilde{E}_1 V, \ldots, -\left(V^T\tilde{E}_0 V\right)^{-1} V^T \tilde{E}_p V\right] \left(V^T \tilde{E}_0 V\right)^{-1} V^T b \\ &= V^T F^m_{k_2,\ldots,k_p}\left[-\tilde{E}_0^{-1}\tilde{E}_1, \ldots, -\tilde{E}_0^{-1}\tilde{E}_p\right] \tilde{E}_0^{-1} b. \end{aligned} \tag{27}$$

$$\begin{aligned} \operatorname{colspan}(V) = \operatorname{span}\Bigg\{ &\bigcup_{m=0}^{m_q} \bigcup_{k_2=0}^{m-(k_p+\cdots k_3)} \cdots \bigcup_{k_p=0}^{m} F^m_{k_2,\ldots,k_p}(M_1,\ldots,M_p)[b_M]_1, \ldots, \\ &\bigcup_{m=0}^{m_q} \bigcup_{k_2=0}^{m-(k_p+\cdots k_3)} \cdots \bigcup_{k_p=0}^{m} F^m_{k_2,\ldots,k_p}(M_1,\ldots,M_p)[b_M]_t \Bigg\}. \end{aligned} \tag{28}$$

$m_q = 1$ and show good accuracy. Using $m_q = 2$ improves the accuracy but generates a larger system. For example, with $m_q = 2$ the order of the produced parameterized model is

$$q = f_{0,p} + f_{1,p} + f_{2,p} = 1 + p + \frac{p(p+1)}{2} = \frac{p^2+3p+2}{2}$$

which implies that a 66th order model will be generated from a problem with $p = 10$ parameters. For larger values of m_q, impractically large models will be generated even for a small number of parameters p.

In terms of computational cost, it is important to make a distinction between the cost of "constructing" the model and the cost of "evaluating" the model. The models constructed by our procedure are extremely small compared to the original systems, therefore, their evaluation cost is also small compared to the construction cost. In particular, when constructing the model, most of the cost is in constructing each of the q columns of matrix V. In particular, generating vectors F^m defined in (24), is the most expensive operation, given that it involves iterative large and dense matrix solves in M_j, and several other large and dense matrix-vector multiplications. In order to make the cost of model computation practical, one can use Krylov subspace iterative methods combined with "fast-methods" [16]–[20] for the required matrix-vector products. Exploiting such well developed techniques, we need to perform $O(n\log(n))$ operations for each column of V. Hence, the total construction cost is $O(qn)$, where q is typically on the order of few hundreds, and n can be as large as hundreds of thousands. When evaluating the model, one needs only solve a small matrix of size q, therefore, the evaluation cost is very low.

VII. Example: A Bus Model Parameterized in the Wires' Spacing

One design consideration for interconnect busses is the tradeoff between:

- wider spacing to reduce propagation delays and crosstalk.
- narrower spacing to reduce area and therefore cost.

In this example, we have used a multiparameter model-order-reduction approach to construct a low-order model of an interconnect bus, parameterized by the wire spacing. The model can be efficiently constructed "on the fly" during the design and can account for the topology of the surrounding interconnect already present in the design. Once produced, the model can be simply evaluated for different values of the main parameter, the wire spacing, in order to determine propagation delay, crosstalk or even detailed step responses.

Our example problem is the bus in Fig. 4, which consists of $N = 16$ parallel wires, with thickness $h = 1.2$ μm, and width $w = 1$ μm. The total length of each wire is $l = 1$ mm. Above and below our bus, we assumed a random collection of interconnect at several layout levels, ranging from a distance of 1 to 5 μm. We have subdivided each wire into 20 equal sections delimited by $n = 21$ nodes. Each section has been modeled with a resistor. Each node has a "grounded capacitor" representing the interaction with upper and lower interconnect levels. In addition, each node has two coupling capacitors to the adjacent wires on the bus. The value of the capacitors was determined

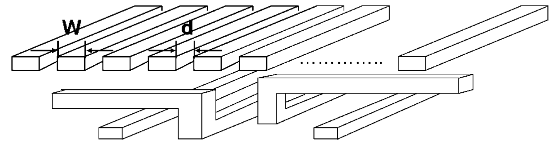

Fig. 4. Sketch of the modeled 16 parallel wires interconnect bus above a random collection of prerouted interconnect at lower layers.

using simple parallel plate formulas. Standard frequency-domain nodal analysis leads to a system of equations of the form

$$\begin{aligned} s\left(C_g + \frac{C_s}{d}\right)v + Gv &= Bv_{\text{in}} \\ v_{\text{out}} &= Cv \end{aligned} \tag{29}$$

where s is the Laplace transform variable, d is the spacing between wires, G is the $n \times n$ nodal conductance matrix. The $n \times n$ matrix C_g is the diagonal nodal matrix associated with the grounded capacitors, and C_s is the sparse nodal matrix associated with the adjacent coupling capacitors. B is the $n \times t$ matrix relating t input voltages v_{in} to the n internal node potentials v, C is a $t \times n$ matrix relating node potentials v to the t output voltages v_{out}. We would like to underline that our model is limited to capturing the behavior of the interconnect, which is linear for almost all practical applications. Our models can then be used in conjunction with any device model, from the most simple linear device model to the most sophisticated spice device model. It is not the purpose of this paper to discuss models for devices, however, just in order to "simulate" our interconnect model, for simplicity we will drive our wires with ideal linear devices having impedance $r_d = 1/g_d$. In general, when g_d is much smaller than the conductance g of a wire section, all the capacitors in the different sections of each wire appear as lumped, and the detailed model presented here is not necessary. A more interesting case is observed when instead g_d is large. In such a case, the wires charge up slowly from the input side of the bus and continue to charge up along the length of the bus. In order to observe this more interesting effect, we chose $g_d \approx g$. All of the wires are left open on the other side.

A. Crosstalk From One Input to all Outputs

When determining the crosstalk generated on all the outputs by a transition on a single input, the input matrix becomes a vector

$$B = b[0\ldots 0 g_d 0 \ldots 0]^T$$

and the output matrix is

$$C = \begin{bmatrix} \ldots 010 \ldots & & & \\ & \ldots 010 \ldots & & \\ & & \ddots & \\ & & & \ldots 01 \end{bmatrix}.$$

The system in (29) has the following parameterized descriptor matrix

$$E\left(s, \frac{1}{d}\right) = sC_g + s\frac{1}{d}C_s + G$$

where we choose to work with parameter $1/d$ instead of parameter d. For frequency s, we choose as expansion point $\bar{s}_1 = \bar{s} = 0$. For the separation, we choose $\bar{s}_2 = 1/d_0 = 1/1\ \mu$m.

$$E\left(s, \frac{1}{d}\right) = G + s\left[C_g + \frac{1}{d_0}C_s\right] + s\left(\frac{\Delta\left(\frac{1}{d}\right)}{\frac{1}{d_0}}\right)\left[\frac{1}{d_0}C_s\right]. \tag{30}$$

Either by identifying terms directly on (30) or by using the formulas in (20)–(21), one can recognize a system as in (19) defining

$$\begin{aligned} \tilde{E}_0 &= G \\ \tilde{E}_1 &= C_g + \frac{1}{d_0}C_s & \tilde{s}_1 &= s \\ \tilde{E}_2 &= \frac{1}{d_0}C_s & \tilde{s}_2 &= s\left(\frac{\Delta\left(\frac{1}{d}\right)}{\frac{1}{d_0}}\right). \end{aligned}$$

The original system for this example has an order of 336 (16 wires $\times 21$ nodes each). We performed a model-order reduction procedure as described in Section V and obtained a small model capturing the transfer functions from one input to all outputs

$$\begin{aligned} \left[\hat{\tilde{E}}_0 + \tilde{s}_1\hat{\tilde{E}}_1 + \tilde{s}_2\hat{\tilde{E}}_2\right]\hat{x} &= \hat{b}u \\ y &= \hat{C}\hat{x} \end{aligned} \tag{31}$$

where

$$\begin{aligned} \hat{\tilde{E}}_0 &= V^T\tilde{E}_0V = V^TGV \\ \hat{\tilde{E}}_1 &= V^T\tilde{E}_1V = V^T\left[C_g + \frac{1}{d_0}C_s\right]V \\ \hat{\tilde{E}}_2 &= V^T\tilde{E}_2V = V^T\left[\frac{1}{d_0}C_s\right]V \\ \hat{b} &= V^Tb \\ \hat{C} &= CV. \end{aligned}$$

The projection matrix V can be constructed such that

$$\mathrm{colspan}(V) = \mathrm{span}\Big\{b_M, M_1b_M, M_2b_M, M_1^2b_M, (M_1M_2 + M_2M_1)b_M, M_2^2b_M, \ldots\Big\},$$

where

$$\begin{aligned} b_M &= \tilde{E}_0^{-1}b = G^{-1}b \\ M_1 &= -\tilde{E}_0^{-1}\tilde{E}_1 = -G^{-1}\left[C_g + \frac{1}{d_0}C_s\right] \\ M_2 &= -\tilde{E}_0^{-1}\tilde{E}_2 = -G^{-1}\left[\frac{1}{d_0}C_s\right]. \end{aligned}$$

A modified Arnoldi algorithm [8] could be used to orthonormalize the columns of V during the matrix construction.

The step response at the end of the wire excited as shown in the top of Fig. 5 is given in the graphs of the same figure. The graphs compare the step responses of the original system (continuous lines) and a reduced model of order three (small crosses) when the spacing distance assumes the values $d = d_0 + \Delta d =$ 0.5, 1, and 10 μm. The model was constructed using a nominal spacing $d_0 = 1\ \mu$m; hence, the error is smaller near $d \approx d_0 = 1\ \mu$m. One can notice that the reduced model can be easily and accurately used to evaluate the step response and propagation delay for any value of parameter d near d_0, by plugging into the reduced model (31). From the reduced model (31), we have readily available not only step responses on the same wire, but also crosstalk step responses from one wire to all the other wires. For example, Fig. 6 shows step responses from the input of wire 4 to the output of wires 4–7. In this figure, we compare again the response of the original system of order 336 (continues curves) with the response of a reduced model order 10 (small crosses) constructed at nominal spacing $d_0 = 1\ \mu$m, but evaluated in this particular figure at spacing $d = 0.5\ \mu$m. Note that the model produced by our procedure is parameterized in the wire spacing, hence, *any* of the such crosstalk responses can be evaluated at *any* spacing. For instance, we show in Fig. 7 the response at the

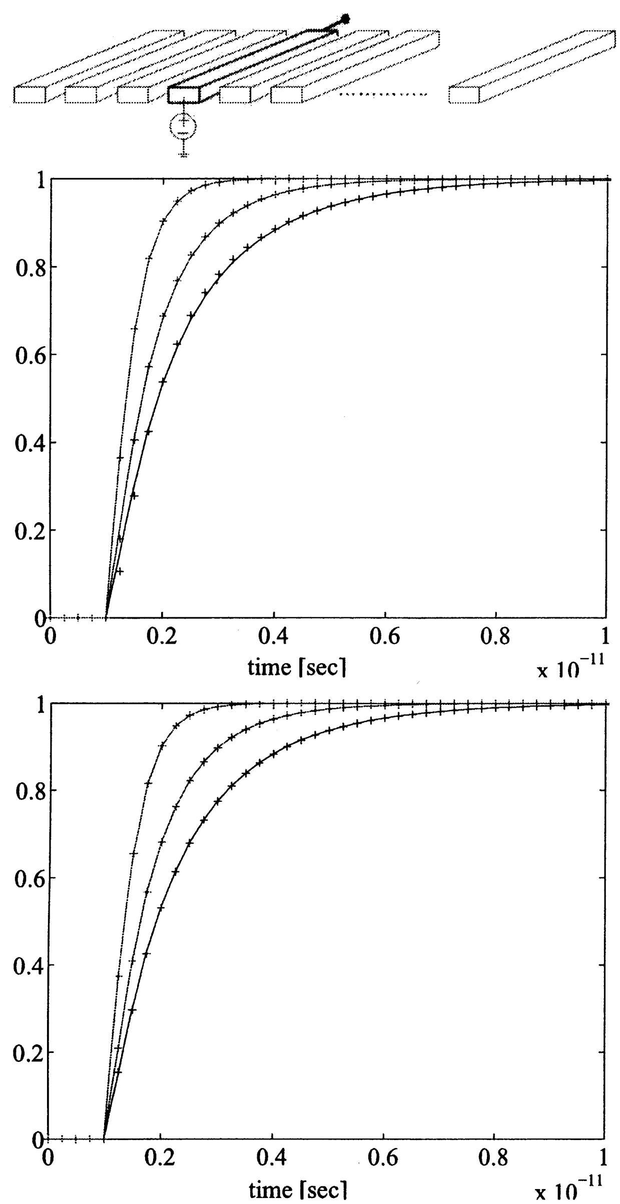

Fig. 5. Responses at the end of wire 4 when a step is applied at the beginning of the same wire. Continuous lines are the response of the original system (order 336). Small crosses are the response of the reduced model, order 3 (top), and order 6 (bottom). The model was constructed using a nominal wire spacing $d_0 = 1\ \mu$m and responses are shown here evaluating it at spacing (from the lowest curves to the highest) $d = d_0 + \Delta d =$ 0.5, 1, and 10 μm.

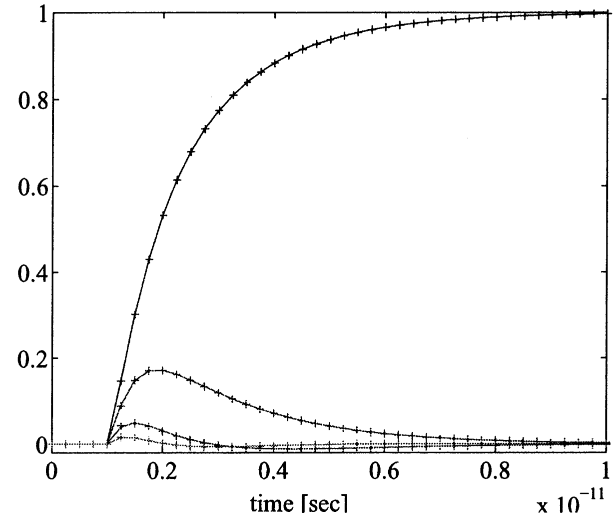

Fig. 6. Responses at the end of wires 4–7 (from highest to lowest curve) when a step is applied at the beginning of wire 4. Continuous lines are the response of the original system (order 336). Small crosses are the response of the reduced model (order 10). The model was constructed using a nominal wire spacing $d_0 = 1\ \mu$m and responses are shown here evaluating it at spacing $d = 0.5\ \mu$m.

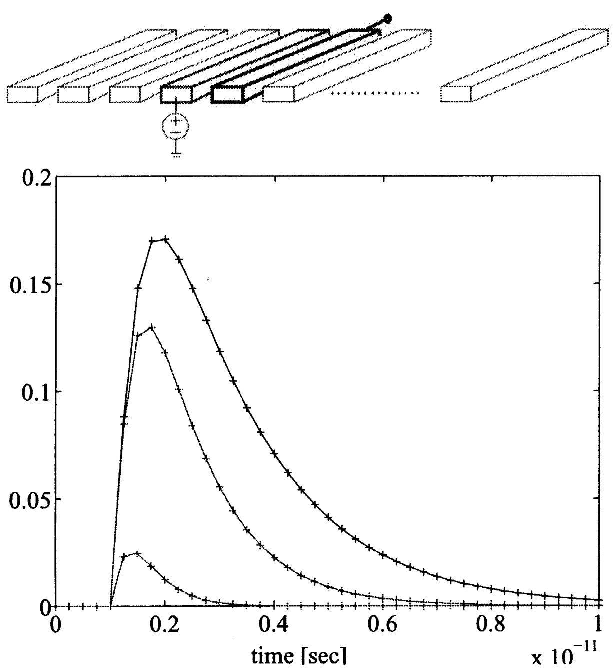

Fig. 7. Crosstalk responses at the end of wire 5, when a step is applied at the beginning of wire 4, for different values of spacing (from highest to lowest curve) $d = d_0 + \Delta d =$ 0.5, 1, and 10 μm.

output of wire 5 when a step waveform is applied at the input of wire 4 for different spacing values, $d = d_0 + \Delta d =$ 0.5, 1, 10 μm.

B. Exploiting the Adjoint Method for Crosstalk From All Inputs to One Output

It is possible to construct, with the same amount of calculation, a model that provides the susceptibility of one output to all inputs. In order to do this, we can use an adjoint method and start from an original system which swaps positions of C and B

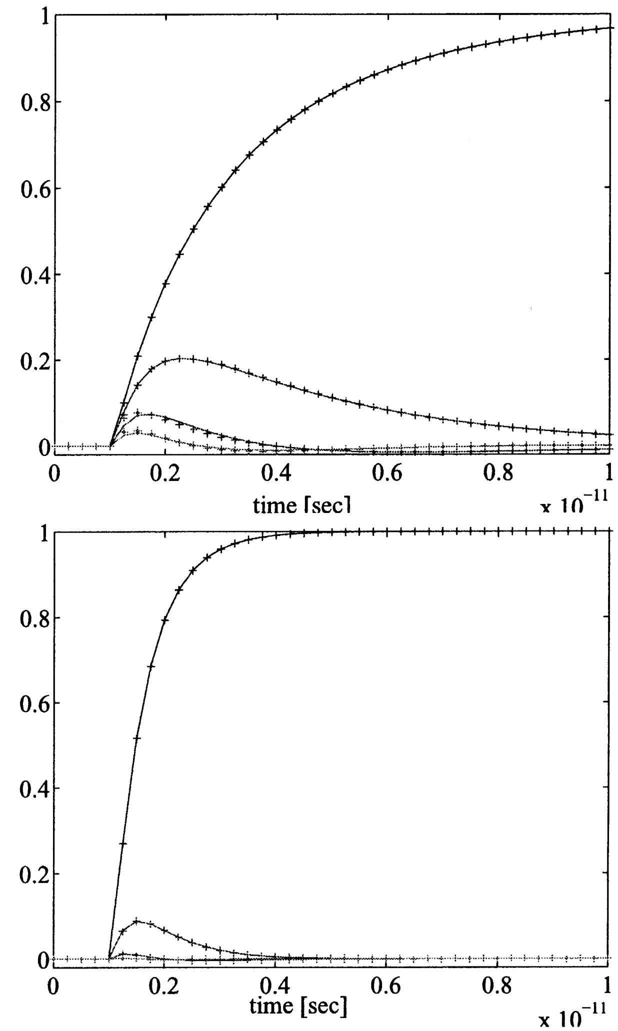

Fig. 8. Adjoint method results: responses at the end of wire 4, when a step is applied at the beginning of wires 4–7 (from highest to lowest curve). Continuous lines are the response of the original system (order 336). Small crosses are the response of the reduced model (order 10). The model was constructed using $d_0 = 1\ \mu$m. The plot on top is for $d = 0.25\ \mu$m. The plot on the bottom is for $d = 2\ \mu$m.

and transposes all system matrices. Note that since we are considering a single output $C \in \mathbf{R}^{1\times n}$ and $C^T \in \mathbf{R}^{n\times 1}$ is a vector

$$\begin{aligned} \left[I - \left(\tilde{s}_1 M_1^T + \tilde{s}_2 M_2^T\right)\right] v' &= C^T v'_{\text{in}} \\ v'_{\text{out}} &= B_M^T v'. \end{aligned} \tag{32}$$

In this case, the columns of the projection operator V will span the Krylov subspace

$$\text{colspan}(V') = \text{span}\Big\{C^T, M_1^T C^T, M_2^T C^T, M_1^T M_1^T C^T, \\ \left(M_1^T M_2^T + M_2^T M_1^T\right) C^T, M_2^T M_2^T C^T, \dots\Big\}$$

or in general

$$\text{colspan}(V') = \text{span}\left\{\bigcup_{m=0}^{m_q}\left(\bigcup_{k=0}^{m} F_k^m(M_1^T, M_2^T)C^T\right)\right\}.$$

In Fig. 8, we show the responses at the end of wire 4 when a step is applied at the beginning of wires 4–7. The model was constructed using a nominal wire spacing $d_0 = 1\ \mu$m. Responses in Fig. 8 (top) are for $d = 0.25\ \mu$m. Responses in Fig. 8 (bottom) are for $d = 2\ \mu$m.

VIII. Example: Bus Model Parameterized in Both Wire Width and Separation

Often, when designing an interconnect bus, one would like to quickly evaluate design tradeoffs originating not only from different wire spacings, but also for different wire widths. Wider wires have lower resistances but use more area and have higher capacitance. The higher capacitance to ground, however, helps improving crosstalk immunity. We show here a procedure that produces small models that can be easily evaluated with respect to propagation delays and crosstalk performance for different values of the two parameters: wire spacing d, and wire width W. As in the case of wire spacing, we constructed models for a given nominal wire width W_0, and then we parameterized in terms of perturbations ΔW. Considering the same bus example with N parallel wires described in Section VII, we can write the equations for the original large parameterized linear system

$$s\left(WC_g' + \frac{C_s}{d}\right)v + WG'v = Bv_{\text{in}}$$
$$v_{\text{out}} = Cv.$$

The system has the following parameterized descriptor matrix

$$E\left(s, \frac{1}{d}, W\right) = sWC_g' + s\frac{1}{d}C_s + WG'$$

where $C_g' = C_g/W$, $G' = G/W$, and C_g and G are as described in Section VII. With respect to the expansion points $\bar{s}_1 = \bar{s}_0 = 0$, $\bar{s}_2 = 1/d_0$, $\bar{s}_3 = W_0$

$$E\left(s, \frac{1}{d}\right) = W_0G' + s\left[W_0C_g' + \frac{1}{d_0}C_s\right] + \left(\frac{\Delta W}{W_0}\right)[W_0G'] + s\left(\frac{\Delta W}{W_0}\right)[W_0C_g'] + s\left(\frac{\Delta\left(\frac{1}{d}\right)}{\frac{1}{d_0}}\right)\left[\frac{1}{d_0}C_s\right]. \quad (33)$$

Either by identifying terms directly on (33) or by using the formulas in (20)–(21), one can recognize a system as in (19) defining

$$\begin{aligned}
\tilde{E}_0 &= W_0G' \\
\tilde{E}_1 &= W_0C_g' + \frac{1}{d_0}C_s \quad \tilde{s}_1 = s \\
\tilde{E}_2 &= W_0G' \qquad \tilde{s}_2 = \frac{\Delta W}{W_0} \\
\tilde{E}_3 &= W_0C_g' \quad \tilde{s}_2 = s\left(\frac{\Delta W}{W_0}\right) \\
\tilde{E}_4 &= \frac{1}{d_0}C_s \quad \tilde{s}_2 = s\left(\frac{\Delta\left(\frac{1}{d}\right)}{\frac{1}{d_0}}\right).
\end{aligned}$$

Following the procedure in Section V, the produced reduced order model is

$$\left[\hat{\tilde{E}}_0 + \tilde{s}_1\hat{\tilde{E}}_1 + \tilde{s}_2\hat{\tilde{E}}_2 + \tilde{s}_3\hat{\tilde{E}}_3 + \tilde{s}_4\hat{\tilde{E}}_4\right]\hat{x} = \hat{B}u$$
$$y = \hat{C}\hat{x} \quad (34)$$

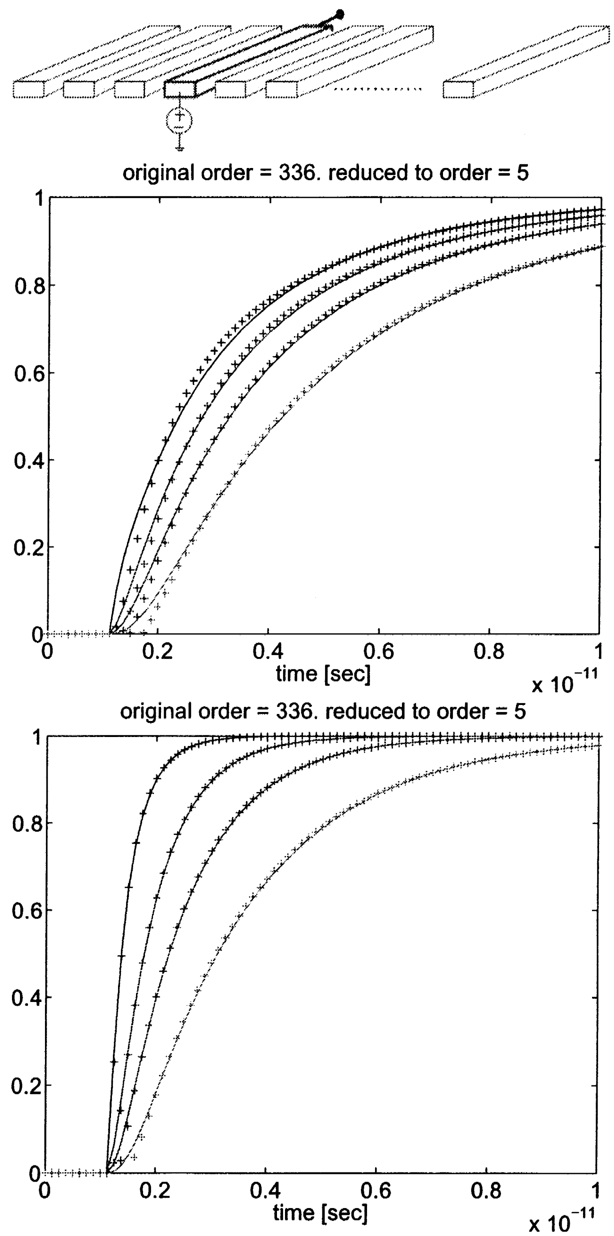

Fig. 9. Original system (continuous curves) versus fifth-order reduced model (small crosses) using both spacing and width parameters. The nominal wire spacing was $d_0 = 1\mu$m and the nominal wire width was $W = 1\ \mu$m.Top: responses at the end of wire 4 due to a step at the beginning of the same wire for different widths (from highest to lowest curve) $W = 0.25$, 2, 4, and 8 μm and for spacing $d = 0.25\ \mu$m. Bottom: same responses but for spacing $d = 2\ \mu$m.

where

$$\begin{aligned}
\hat{\tilde{E}}_0 &= V^T\tilde{E}_0V = V^*W_0G'V \\
\hat{\tilde{E}}_1 &= V^T\tilde{E}_1V = V^T\left[W_0C_g' + \frac{1}{d_0}C_s\right]V \\
\hat{\tilde{E}}_2 &= V^T\tilde{E}_2V = V^T[W_0G']V \\
\hat{\tilde{E}}_3 &= V^T\tilde{E}_3V = V^T\left[W_0C_g'\right]V \\
\hat{\tilde{E}}_4 &= V^T\tilde{E}_4V = V^T\left[\frac{1}{d_0}C_s\right]V \\
\hat{B} &= V^TB \\
\hat{C} &= CV.
\end{aligned}$$

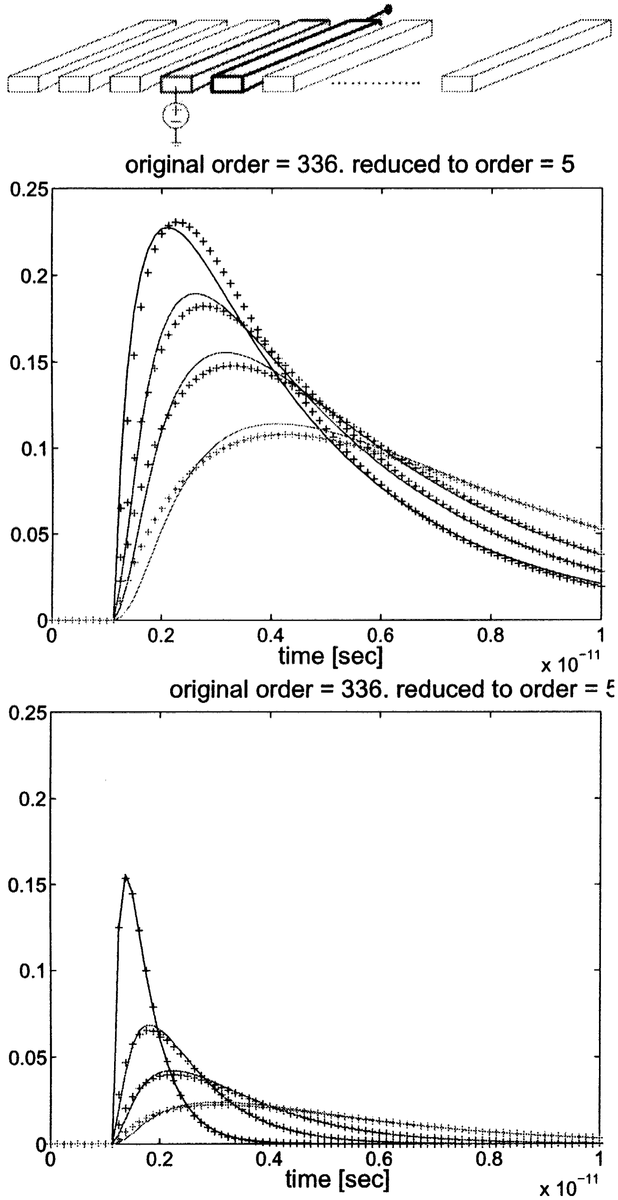

Fig. 10. Original system (continuous curves) versus 5th order reduced model (small crosses) using both spacing and width parameters. The nominal wire spacing was $d_0 = 1\ \mu$m and the nominal wire width was $W = 1\ \mu$m. Top: crosstalk at the end of wire 5 due to a step at the beginning of wire 4. Curves correspond to widths (from highest curve to lowest) $W = 0.25$, 2, 4, and 8 μm and spacing is $d = 0.25\ \mu$m. Bottom: same crosstalk responses but for spacing $d = 2\ \mu$m.

The projection matrix V can be constructed for instance for a single input case ($B = b \in \mathbf{R}^{n\times 1}$) as shown in (26) where

$$
\begin{aligned}
b_M &= \tilde{E}_0^{-1} b = (W_0 G')^{-1} b \\
M_1 &= -\tilde{E}_0^{-1}\tilde{E}_1 = -(W_0 G')^{-1}\left[W_0 C_g' + \frac{1}{d_0} C_s\right] \\
M_2 &= -\tilde{E}_0^{-1}\tilde{E}_2 = -(W_0 G')^{-1}\left[W_0 G'\right] \\
M_3 &= -\tilde{E}_0^{-1}\tilde{E}_3 = -(W_0 G')^{-1}\left[W_0 C_g'\right] \\
M_4 &= -\tilde{E}_0^{-1}\tilde{E}_4 = -(W_0 G')^{-1}\left[\frac{1}{d_0} C_s\right].
\end{aligned}
$$

A modified Arnoldi algorithm [8] could be used to orthonormalize the columns of V during the matrix construction.

In Figs. 9 and 10, we compare the step and crosstalk responses of the original system to the reduced and parameterized model obtained using a Krylov subspace of order $q = 5$. This corresponds to choosing $m_q = 1$ in (26), or in other words it corresponds to constructing a reduced model that matches the original model up to one moment (or derivative) for each parameter s_j. The model was constructed using a nominal spacing $1/d_0 = 1/1\ \mu$m and nominal wire width $W_0 = 1\ \mu$m. The key point is that this parameterized model can be rapidly evaluated for any value of spacing and wire width, for instance for a fast and accurate tradeoff design optimization procedure.

IX. Conclusion

In this paper, we described an approach for generating geometrically parameterized integrated circuit interconnect models that are efficient enough for use in interconnect synthesis. The model generation approach presented is automatic, and is based on series expansion of the parameter dependence followed by single or multiparameter model-reduction. The effectiveness of the techniques described was tested using a multiline bus example in two different settings. In the first setting, the model reduction approach was used to automatically generate, from an integral equation-based capacitance-extraction algorithm, second-order models for the dependence of self and coupling capacitances on line separation. In the second setting, multiparameter-model reduction was used to generate, from a formula-based capacitance and resistance-extraction algorithm, high-order models for the dependence of delay and cross-talk on line separation and conductor width. The experimental results clearly demonstrated that the reduction strategies generated models that were accurate over a wide range of geometric variation.

It should be noted, however, that there are closed-form analytical models which relate geometric parameters to self and coupling capacitances, and the model-reduction approaches presented herein are unlikely to be as efficient. However, the methods presented here are potentially more accurate, and certainly more automatic and more flexible. In addition, there are many potential issues that can lead to new contributions in this field. The multiparameter method was tested using only resistor-capacitor interconnect models, and accuracy issues may arise when inductance is included. We also did not investigate using multipoint moment matching, which could be a better choice given the range of the parameters is often known *a priori*. In addition, the multiparameter reduction method can become quite expensive when a large accuracy is required and the model has a large number of parameters, so the method would not generate a very efficient model if each wire pair spacing in a 16 wire bus was treated individually. Finally, there are some interesting error bounds in [4], and these results could be applied to automatically select the reduction order.

$$(V^T\tilde{E}_0V)^{-1}V^Tb = V^T\tilde{E}_0^{-1}b = V^TF^0_{k_2,\ldots,k_p}\left[-\tilde{E}_0^{-1}\tilde{E}_1,\ldots,-\tilde{E}_0^{-1}\tilde{E}_p\right]\tilde{E}_0^{-1}b \tag{35a}$$

$$\begin{aligned}[]&[\tilde{s}_1M_1+\cdots+\tilde{s}_pM_p]^{m-1}\\ &\quad=\sum_{k_2=0}^{(m-1)-(k_3+\cdots+k_p)}\cdots\sum_{k_{p-1}=0}^{(m-1)-k_p}\sum_{k_p=0}^{m-1}\left\{\left[F^{m-1}_{k_2,\ldots,k_p}(M_1,\ldots,M_p)\right]\tilde{s}_1^{(m-1)-(k_2+\cdots+k_p)}\tilde{s}_2^{k_2}\cdots\tilde{s}_p^{k_p}\right\}.\end{aligned} \tag{35}$$

$$\begin{aligned}[]&[\tilde{s}_1M_1+\cdots+\tilde{s}_pM_p]^{m}\\ &\quad=[\tilde{s}_1M_1+\cdots+\tilde{s}_pM_p]\sum_{k_2=0}^{(m-1)-(k_3+\cdots+k_p)}\cdots\sum_{k_{p-1}=0}^{(m-1)-k_p}\sum_{k_p=0}^{m-1}\left\{\left[F^{m-1}_{k_2,\ldots,k_p}(M_1,\ldots,M_p)\right]\tilde{s}_1^{(m-1)-(k_2+\cdots+k_p)}\tilde{s}_2^{k_2}\ldots\tilde{s}_p^{k_p}\right\}\end{aligned} \tag{36}$$

$$\begin{aligned}&=\sum_{k_2=0}^{(m-1)-(k_3+\cdots+k_p)}\cdots\sum_{k_{p-1}=0}^{(m-1)-k_p}\sum_{k_p=0}^{m-1}\left\{\tilde{s}_1M_1F^{m-1}_{k_2,\ldots,k_p}(M_1,\ldots,M_p)\tilde{s}_1^{(m-1)-(k_2+\cdots+k_p)}\tilde{s}_2^{k_2}\cdots\tilde{s}_p^{k_p}+\cdots\right.\\ &\qquad\left.+\tilde{s}_pM_pF^{m-1}_{k_2,\ldots,k_p-1}(M_1,\ldots,M_p)\tilde{s}_1^{m-(k_2+\cdots+k_p)}\tilde{s}_2^{k_2}\ldots\tilde{s}_p^{k_p-1}\right\}\\ &=\sum_{k_2=0}^{(m-1)-(k_3+\cdots+k_p)}\cdots\sum_{k_{p-1}=0}^{(m-1)-k_p}\sum_{k_p=0}^{m-1}\left\{\left[M_1F^{m-1}_{k_2,\ldots,k_p}(M_1,\ldots,M_p)+\cdots+M_pF^{m-1}_{k_2,\ldots,k_p-1}(M_1,\ldots,M_p)\right]\right.\\ &\qquad\left.\times\tilde{s}_1^{m-(k_2+\cdots+k_p)}\tilde{s}_2^{k_2}\ldots\tilde{s}_p^{k_p}\right\}.\end{aligned} \tag{37}$$

$$\begin{aligned}&\hat{F}^m_{k_2,\ldots,k_p}\left[-(V^T\tilde{E}_0V)^{-1}V^T\tilde{E}_1V,\ldots,-(V^T\tilde{E}_0V)^{-1}V^T\tilde{E}_pV\right](V^T\tilde{E}_0V)^{-1}V^Tb\\ &\quad=\left[(V^T\tilde{E}_0V)^{-1}V^T\tilde{E}_1V\hat{F}^{m-1}_{k_2,\ldots,k_p}(-(V^T\tilde{E}_0V)^{-1}V^T\tilde{E}_1V,\ldots,-(V^T\tilde{E}_0V)^{-1}V^T\tilde{E}_pV)+\cdots\right.\\ &\qquad\left.+(V^T\tilde{E}_0V)^{-1}V^T\tilde{E}_pV\hat{F}^{m-1}_{k_2,\ldots,k_p-1}(-(V^T\tilde{E}_0V)^{-1}V^T\tilde{E}_1V,\ldots,-(V^T\tilde{E}_0V)^{-1}V^T\tilde{E}_pV)\right](V^T\tilde{E}_0V)^{-1}V^Tb\end{aligned} \tag{38}$$

$$\begin{aligned}&=\left[(V^T\tilde{E}_0V)^{-1}V^T\tilde{E}_1VV^TF^{m-1}_{k_2,\ldots,k_p}(-\tilde{E}_0^{-1}\tilde{E}_1,\ldots,-\tilde{E}_0^{-1}\tilde{E}_p)+\cdots+(V^T\tilde{E}_0V)^{-1}V^T\tilde{E}_pVV^TF^{m-1}_{k_2,\ldots,k_p-1}\right.\\ &\qquad\left.\times(-\tilde{E}_0^{-1}\tilde{E}_1,\ldots,-\tilde{E}_0^{-1}\tilde{E}_p)\right]\tilde{E}_0^{-1}b\\ &=\left[(V^T\tilde{E}_0V)^{-1}V^T\tilde{E}_1F^{m-1}_{k_2,\ldots,k_p}(-\tilde{E}_0^{-1}\tilde{E}_1,\ldots,-\tilde{E}_0^{-1}\tilde{E}_p)+\cdots\right.\\ &\qquad\left.+(V^T\tilde{E}_0V)^{-1}V^T\tilde{E}_pF^{m-1}_{k_2,\ldots,k_p-1}(-\tilde{E}_0^{-1}\tilde{E}_1,\ldots,-\tilde{E}_0^{-1}\tilde{E}_p)\right]\tilde{E}_0^{-1}b\end{aligned} \tag{39}$$

$$=(V^T\tilde{E}_0V)^{-1}V^T\left[\tilde{E}_1F^{m-1}_{k_2,\ldots,k_p}\times(-\tilde{E}_0^{-1}\tilde{E}_1,\ldots,-\tilde{E}_0^{-1}\tilde{E}_p)+\cdots+\tilde{E}_pF^{m-1}_{k_2,\ldots,k_p-1}(-\tilde{E}_0^{-1}\tilde{E}_1,\ldots,-\tilde{E}_0^{-1}\tilde{E}_p)\right]\tilde{E}_0^{-1}b \tag{40}$$

$$=V^TF^m_{k_2,\ldots,k_p}\left[-\tilde{E}_0^{-1}\tilde{E}_1,\ldots,-\tilde{E}_0^{-1}\tilde{E}_p\right]\tilde{E}_0^{-1}b. \tag{41}$$

APPENDIX

A. Proof of Lemma 1

Lemma 1 can be shown by induction on m. For $m = 0$, we can easily verify that

$$[\tilde{s}_1 M_1 + \cdots + \tilde{s}_p M_p]^0 = 1.$$

Let us now assume for $m - 1$ that (35) holds. In order to show that the property holds for m, we can first write (36). Multiplying and collecting the terms with the same powers of $\tilde{s}_1, \ldots, \tilde{s}_p$, we obtain (37), which proves that the statement holds for m.

B. Proof of Lemma 2

As from [8], if $z \in \mathrm{colspan}(V)$, then there must exist a vector y such that $Vy = z$. Substituting, $VV^T z = VV^T Vy = Vy = z$.

C. Proof of Lemma 3

As from [8], we need to show that $y = V^T \tilde{E}_0^{-1} z$ is a solution for the linear system $(V^T \tilde{E}_0 V)y = V^T z$. Substituting, $(V^T \tilde{E}_0 V)y = (V^T \tilde{E}_0 V)V^T \tilde{E}_0^{-1} z$. Since $\tilde{E}_0^{-1} z \in \mathrm{colspan}(V)$ from Lemma 2 we have that $V^T \tilde{E}_0 V V^T \tilde{E}_0^{-1} z = V^T \tilde{E}_0 \tilde{E}_0^{-1} z = V^T z$.

D. Proof of Lemma 4

A proof is given in this paper by induction on the order m of the coefficient. First, let us prove the statement in the lemma for $m = 0$, i.e.,

$$\hat{F}^0_{k_2,\ldots,k_p}\left[-\left(V^T\tilde{E}_0V\right)^{-1}V^T\tilde{E}_1V,\ldots,\right.$$
$$\left.-\left(V^T\tilde{E}_0V\right)^{-1}V^T\tilde{E}_pV\right]$$
$$\cdot\left(V^T\tilde{E}_0V\right)^{-1}V^Tb = I\left(V^T\tilde{E}_0V\right)^{-1}V^Tb.$$

Since $\tilde{E}_0^{-1} b \in \mathrm{colspan}(V)$, from Lemma 3 we have (35a). (See equation (35a) at the top of the previous page.) This concludes the proof for $m = 0$. Let us now assume that the statement is correct for order $m - 1$ and let us show that this implies it is correct for order m. From the recursive definition formula (24), we have (38), Using the inductive hypothesis on order $m-1$ for each of the terms in the summation we have (39). Using Lemma 2 on each of the terms of the summation we have (40). Since

$$\tilde{E}_0^{-1}\left[\tilde{E}_1F^{m-1}_{k_2,\ldots,k_p}\left(\tilde{E}_0^{-1}\tilde{E}_1,\ldots,\tilde{E}_0^{-1}\tilde{E}_p\right)+\cdots\right.$$
$$\left.+\tilde{E}_pF^{m-1}_{k_2,\ldots,k_p-1}\left(\tilde{E}_0^{-1}\tilde{E}_1,\ldots,\tilde{E}_0^{-1}\tilde{E}_p\right)\right]\tilde{E}_0^{-1}b$$
$$=F^m_{k_2,\ldots,k_p}\left[\tilde{E}_0^{-1}\tilde{E}_1,\ldots,\tilde{E}_0^{-1}\tilde{E}_p\right]\tilde{E}_0^{-1}b$$
$$=F^m_{k_2,\ldots,k_p}\left[\tilde{E}_0^{-1}\tilde{E}_1,\ldots,\tilde{E}_0^{-1}\tilde{E}_p\right]b_M\in\mathrm{colspan}(V)$$

we can use Lemma 3 and obtain (41). Note that the hypothesis for Lemmas 2 and 3 in this context hold only for $m = 0, 1, \ldots, m_q$. Hence, (27) holds only for $m = 0, 1, \ldots, m_q$. This concludes the proof of Lemma 4.

E. Proof of Theorem 1

The transfer function of the system in (19) for a single input case ($B = b \in \mathbf{R}^{n\times 1}$) is given by (42). Similarly, the transfer function of the system in (22) is given by (43). Using first Lemma 4, then Lemma 2, we can see that each moment of the reduced model transfer function expansion (43) matches the corresponding moment of the original transfer function expansion (42)

$$C\hat{F}^m_{k_2,\ldots,k_p}\left[-\left(V^T\tilde{E}_0V\right)^{-1}V^T\tilde{E}_1V,\ldots,\right.$$
$$\left.-\left(V^T\tilde{E}_0V\right)^{-1}V^T\tilde{E}_pV\right]\left(V^T\tilde{E}_0V\right)^{-1}V^Tb$$
$$=CVV^TF^m_{k_2,\ldots,k_p}\left(-\tilde{E}_0^{-1}\tilde{E}_1,\ldots,-\tilde{E}_0^{-1}\tilde{E}_p\right)\tilde{E}_0^{-1}b$$
$$=CF^m_{k_2,\ldots,k_p}\left(-\tilde{E}_0^{-1}\tilde{E}_1,\ldots,-\tilde{E}_0^{-1}\tilde{E}_p\right)\tilde{E}_0^{-1}b$$
$$=CF^m_{k_2,\ldots,k_p}\left(-\tilde{E}_0^{-1}\tilde{E}_1,\ldots,-\tilde{E}_0^{-1}\tilde{E}_p\right)b_M.$$

Note that Lemmas 2 and 3 in this context hold only for the first q moments, corresponding to $m = 0, 1, \ldots, m_q$. Hence, only those moments are guaranteed to be matched.

$$H = C\left[I-(\tilde{s}_1M_1+\cdots+\tilde{s}_pM_p)\right]^{-1}\tilde{E}_0^{-1}b$$
$$=\sum_{m=0}^{\infty}\sum_{k_2=0}^{m-(k_3+\cdots+k_p)}\cdots\sum_{k_{p-1}=0}^{m-k_p}\sum_{k_p=0}^{m}\left\{\left[CF^m_{k_2,\ldots,k_p}(M_1,\ldots,M_p)b_M\right]\tilde{s}_1^{m-(k_2+\cdots+k_p)}\tilde{s}_2^{k_2}\ldots\tilde{s}_p^{k_p}\right\} \tag{42}$$

$$\hat{H} = CV\left\{I-\left[\tilde{s}_1(V^T(-\tilde{E}_0)V)^{-1}V^T\tilde{E}_1V+\cdots+\tilde{s}_p(V^T(-\tilde{E}_0)V)^{-1}V^T\tilde{E}_pV\right]\right\}^{-1}(V^T\tilde{E}_0V)^{-1}V^Tb$$
$$=\sum_{m=0}^{\infty}\sum_{k_2=0}^{m-(k_3+\cdots+k_p)}\cdots\sum_{k_{p-1}=0}^{m-k_p}\sum_{k_p=0}^{m}\left\{\left[CV\hat{F}^m_{k_2,\ldots,k_p}\left(-(V^T\tilde{E}_0V)^{-1}V^T\tilde{E}_1V,\ldots,-(V^T\tilde{E}_0V)^{-1}V^T\tilde{E}_pV\right)\right.\right.$$
$$\left.\left.\times(V^T\tilde{E}_0V)^{-1}V^Tb\right]\tilde{s}_1^{m-(k_2+\cdots+k_p)}\tilde{s}_2^{k_2}\ldots\tilde{s}_p^{k_p}\right\}. \tag{43}$$

F. Proof of Lemma 5

The number $f_{m,p}$ of coefficients of order m, for a system with p parameters, can be obtained by induction

$$f_{m,p} = \begin{cases} 1, & \text{if } m = 0, \\ \sum_{k=1}^{p} f_{m-1,k}, & \text{if } m > 0 \end{cases}$$

or equivalently

$$f_{m,p} = \binom{m+p-1}{m} = \binom{m+p-1}{p-1} = f_{p-1,m+1} = \frac{(m+p-1)!}{m!(p-1)!}.$$

[See equation (42) and (43) at the bottom of the previous page.] Using, then, the asymptotic approximation [21] for the Gamma Function $\Gamma(z) = (z-1)!$, one obtains

$$f_{m,p} = \frac{\Gamma(m+p)}{\Gamma(m+1)\Gamma(p)} \approx \frac{e}{\sqrt{2\pi}} \frac{(m+p)^{m+p-1/2}}{m^{m+1/2} p^{p-1/2}}.$$

Observing that for most practical problems $m \ll p$, we have

$$f_{m,p} = O\left(\frac{p^m}{m^{m+1/2}}\right).$$

The order q of the produced parameterized reduced system is then

$$q = \sum_{m=0}^{m_q} f_{m,p} = O(m_q f_{m,q}) = O\left(\frac{p^{m_q}}{m_q^{m_q - 1/2}}\right).$$

Acknowledgment

The authors would like to thank J. H. Lee, X. Hu, and D. Willis for correcting many typos while reviewing a preprint version of this article, and the prototype Matlab code for this work.

References

[1] Y. Liu, L. T. Pileggi, and A. J. Strojwas, "Model order-reduction of RCL interconnect including variational analysis," in *Proc. ACM/IEEE Design Automation Conf.*, New Orleans, LA, June 1999, pp. 201–206.

[2] P. Heydari and M. Pedram, "Model reduction of variable-geometry interconnects using variational spectrally-weighted balanced truncation," in *Proc. IEEE/ACM Int. Conf. Computer-Aided Design*, San Jose, CA, Nov. 2001.

[3] S. Pullela, N. Menezes, and L. T. Pileggi, "Moment-sensitivity-based wire sizing for skew reduction in on-chip clock nets," *IEEE Trans. Computer-Aided Design*, vol. 16, pp. 210–215, Feb. 1997.

[4] C. Prud'homme, D. Rovas, K. Veroy, Y. Maday, A. T. Patera, and G. Turinici, "Reliable real-time solution of parametrized partial differential equations: Reduced-basis output bounds methods," *J. Fluids Eng.*, 2002.

[5] K. Gallivan, E. Grimme, and P. Van Dooren, "Asymptotic waveform evaluation via a Lanczos method," *Appl. Math. Lett.*, vol. 7, no. 5, pp. 75–80, 1994.

[6] P. Feldmann and R. W. Freund, "Reduced-order modeling of large linear subcircuits via a block Lanczos algorithm," in *Proc. 32nd ACM/IEEE Design Automation Conf.*, San Francisco, CA, June 1995, pp. 474–479.

[7] K. J. Kerns, I. L. Wemple, and A. T. Yang, "Stable and efficient reduction of substrate model networks using congruence transforms," in *Proc. IEEE/ACM Int. Conf. Computer-Aided Design*, San Jose, CA, Nov. 1995, pp. 207–214.

[8] E. Grimme, "Krylov projection methods for model reduction," Ph.D. dissertation, Coordinated-Science Laboratory, Univ. of Illinois, Urbana-Champaign, 1997.

[9] I. M. Elfadel and D. D. Ling, "A block Arnoldi algorithm for multipoint passive model-order reduction of multiport RLC networks," in *Proc. IEEE/ACM Int. Conf. Computer-Aided Design*, Nov. 1997.

[10] A. Odabasioglu, M. Celik, and L. T. Pileggi, "PRIMA: Passive reduced-order interconnect macromodeling algorithm," *IEEE Trans. Computer-Aided Design*, vol. 17, pp. 645–654, Aug. 1998.

[11] L. M. Silveira, M. Kamon, I. Elfadel, and J. White, "Coordinate-transformed Arnoldi algorithm for generating guarantee stable reduced-order models of RLC," *Comput. Methods Appl. Mech. Eng.*, vol. 169, no. 3–4, pp. 377–389, 1999.

[12] J. E. Bracken, D. K. Sun, and Z. Cendes, "Characterization of electromagnetic devices via reduced-order models," *Comput. Methods Appl. Mech. Eng.*, vol. 169, no. 3–4, pp. 311–330, 1999.

[13] A. C. Cangellaris and L. Zhao, "Passive reduced-order modeling of electromagnetic systems," *Comput. Methods Appl. Mech. Eng.*, vol. 169, no. 3–4, pp. 345–358, 1999.

[14] D. S. Weile, E. Michielssen, E. Grimme, and K. Gallivan, "A method for generating rational interpolant reduced order models of two-parameter linear systems," *Appl. Math. Lett.*, vol. 12, pp. 93–102, 1999.

[15] J. R. Phillips, E. Chiprout, and D. D. Ling, "Efficient full-wave electromagnetic analysis via model-order reduction of fast integral transforms," in *33rd ACM/IEEE Design Automation Conf.*, Las Vegas, Nevada, June 1996, pp. 377–382.

[16] K. Nabors and J. White, "Fastcap: A multipole accelerated 3-d capacitance extraction program," *IEEE Trans. Computer-Aided Design*, vol. 10, pp. 1447–1459, Nov. 1991.

[17] M. Kamon, M. J. Tsuk, and J. K. White, "FASTHENRY: A multipole-accelerated 3-D inductance extraction program," *IEEE Trans. Microwave Theory Tech/*, vol. 42, pp. 1750–1758, Sept. 1994.

[18] J. R. Phillips and J. White, "A precorrected-FFT method for electrostatic analysis of complicated 3-D structures," *IEEE Trans. Computer-Aided Design*, vol. 16, pp. 1059–1072, Oct. 1997.

[19] J. Tausch and J. White, "A multiscale method for fast capacitance extraction," in *Proc. IEEE/ACM Design Automation Conf.*, New Orleans, LA, June 1999, pp. 537–542.

[20] S. Kapur and D. Long, "Large scale capacitance calculations," in *Proc. IEEE/ACM Design Automation Conf.*, Los Angeles, CA, June 2000, pp. 744–749.

[21] M. Abramowitz and I. A. Stegun, *Handbook of Mathematical Functions With Formulas, Graphs, and Mathematical Tables*. Washington, DC: U.S. Gov. Printong Office, 1972.

Luca Daniel (S'98–M'03) received the Laurea degree (*summa cum laude*) in electronic engineering from the "Universita' di Padova," Italy, in 1996, and the Ph.D. degree in electrical engineering from the University of California, Berkeley, in 2003.

He is presently an Assistant Professor in the Department of Electrical Engineering and Computer Science, Massachusetts Institute of Technology (MIT), Cambridge. In 1997, he collaborated with STMicroelectronics Berkeley Laboratories, Berkeley, CA. In 1998, he was with HP Research Labs, Palo Alto, CA. In 2001, he was with Cadence Berkeley Laboratories, Berkeley, CA. His research interests include model order reduction, parasitic extraction, electromagnetic interference, mixed-signal and RF circuit design, power electronics, MEM's design and fabrication.

Dr. Daniel received the "1999 IEEE TRANSACTIONS ON POWER Electronic Prize Paper Award." He has also received four best paper awards in conferences, the SRC International Graduate Fellowship, and the 2001 Bernard Friedman Memorial Prize in Applied Mathematics, from the Department of Mathematics from the University of California at Berkeley, for "demonstrated research ability in applied mathematics."

Ong Chin Siong received the B.Eng. degree in electrical engineering from the National University of Singapore (NUS), Singapore, in 2000, and the M.Eng. degree in high-performance computing in engineered systems from the Singapore–MIT Alliance, NUS, in 2002.

He is currently working as an Engineer, developing Virtual Private Network with Digisafe Pte Ltd.

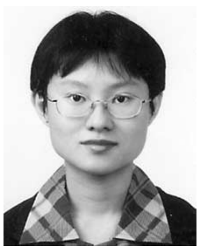

Low Sok Chay received the B.S. degree in computational science and mathematics and the M.Eng. degree in high-performance computation in engineered systems from the National University of Singapore, Singapore, in 2000 and 2002, respectively.

She is currently working as an Operations Analyst with the Defense Science and Technology Agency, Singapore.

Kwok Hong Lee a valued colleague, passed away before publication of this paper. He was an active researcher in computational mechanics, a Vice-Dean of engineering and an Associate Professor in mechanical engineering at the National University of Singapore, Singapore.

Jacob White (A'88) received the B.S. degree from the Massachusetts Institute of Technology, Cambridge, in 1980, and the S.M. and Ph.D. degrees from the University of California, Berkeley, in 1983 and 1985, respectively, all in electrical engineering and computer science.

He was with the IBM T. J. Watson Research Center from 1985 to 1987, was the Analog Devices Career Development Assistant Professor at the Massachusetts Institute of Technology from 1987 to 1989, and was a 1988 Presidential Young Investigator. He is currently a Professor at the Massachusetts Institute of Technology and an Associate Director of the Research Laboratory of Electronics. His current research interests are in numerical algorithms for problems in circuit, interconnect and microelectromechanical system design.

Prof. White was an Associate Editor of the IEEE TRANSACTIONS ON COMPUTER-AIDED DESIGN, from 1992 until 1996, and was Technical Program Chair of the International Conference on Computer-Aided Design in 1998.